J. Violin Soc. Am.: VSA Papers • Summer 2007 • Vol. XXI, No. 1

Surprising Regularity between Plate Modes 2 and 5 and the B1 Corpus Modes: Part I

GEORGE BISSINGER

East Carolina University, Greenville, NC 27858
bissingerg@ecu.edu

Abstract

Martin Schleske noted in 1996 that plate tuning hardly affected corpus "signature" mode frequencies. A simplified heuristic mechanical sandwich (top-ribs-back) B1-ZOM model developed here attributes this lack of dependence to rib stiffness significantly exceeding plate stiffness when the violin is glued together (consistent with a rib-plate stiffness ratio estimate that assumed both were flat plates). Two of these corpus modes, the 1st corpus bending modes $B1^-$ and $B1^+$, are especially significant because they are the only corpus modes to radiate strongly in the open string pitch region. Suggestive plate and corpus mode geometries from modal analysis data provide a plausible path toward understanding the dependence of the B1 modes on rib stiffness and plate modes 2 and 5. A reanalysis of Schleske's data in combination with VIOCADEAS data for nine violins with known plate mode frequencies uncovered a strong statistical correlation between: a) the ratio $\Delta B1/\Delta 5\text{-}2$ of the frequency difference $\Delta B1$ between the $B1^+$ and $B1^-$ modes and the averaged frequency difference $\Delta 5\text{-}2$ between plate modes 2 and 5, and b) the B1 mode frequency ratio and $\Delta B1$ (now for 17 violins), when these are plotted vs. $\Delta B1$.

John Schelleng [1] made the following somewhat casual remark in 1968:

> Traditionally with tap tones, more recently with electronic excitation, the frequencies and character of resonances have been used for . . . [guidance during violin construction]. It seems likely that through neglect of their geometric properties we have allowed a source of information to go to waste.

He further stated that he was unaware of any serious attempt to understand these geometric properties.

Modern modal analysis techniques (combined with traditional Chladni patterns, employed extensively only since the 1960s) that give not only the mode frequencies but also shapes, have given us the opportunity to follow up on his suggestion.[1] We will try to exploit these geometric aspects to the fullest to extract relationships between plate mode frequencies and shapes, commonly gathered by makers who use Chladni patterns, and corpus mode shapes. Specifically, we have examined—in a statistical way—relationships between the top and back plate modes 2 and 5 and the 1st corpus bending modes $B1^-$ and $B1^+$ (B1 modes), suggested by a heuristic physical model, for two entirely different sets of experimental data.

Why do we single out just the B1 modes here? There are a number of good reasons:

1. In the open string pitch region there are only three to four modes that radiate strongly: A0, the compliant wall version of the Helmholtz cavity resonance (always important acoustically), A1 (sometimes important), the 1st longitudinal cavity mode that must induce corpus motion to radiate, and $B1^-$ and $B1^+$, the 1st corpus bending modes (collectively labeled B1; relative strengths vary violin to violin but at least one will radiate strongly). Weak (relative) response in this region is consistent with poor violins.
2. Before detailed knowledge of the modes was available, one bowed violin test (Saunders Loudness plot [2]) using a sound level meter

always showed a large peak in loudness called the "main wood" resonance in the pitch region of the A-string. This peak—due to $B1^-$ and $B1^+$—was used by Schelleng in scaling the violin resonance properties into other pitch ranges (the violin octet) [3, 4].

3. Dünnwald [5] published a summary analysis of acoustic response curves for a large number of violins of varying quality. One figure stood out especially—a three-part plot of 10 Old Italian, 10 master violinmakers, and 10 factory violins, each subplot with all 10 response curves overlaid—showing a seeming regularity for Old Italian violins that was missing in the other groups.
4. Modal analysis provides some suggestive geometry relationships.

An envelope version of this Dünnwald figure, with added notations based on his acoustic characterizations, is shown in Fig. 1. What is immediately apparent is the regularity in frequency placement of $B1^-$ and $B1^+$ in the 10-Old-Italian envelope curve. Does such B1 mode *orderliness* imply some means these makers had to get such consistent frequency placement?

If achieving Old Italian sound is important to a modern maker, then modern violin response curves logically should bear a strong resemblance to the Old Italian ones. How can this be done? Here we address that lowest part of the curve where the "signature" modes are always recognizable and look only at how a maker can approach placing $B1^-$ near 440 Hz and $B1^+$ near 520 Hz (as in the Old Italian curves—although other choices are *apropos*), using just two specific bending modes of the top and back plates, modes 2 and 5.

Our presentation splits into two parts: Part I will look at the way the top and back plate substructure modes migrate to the corpus, the influence of the ribs, a hugely simplified mechanical sandwich (top+ribs+back) model of the violin, finding plate-corpus mode correlations using scatter plots,[2] and solving trendline[3] equations to predict B1 mode frequencies in terms of mode 2 and 5 frequencies.

Part II, to be published in the next issue of *VSA Papers*, starts pretty much where Part I leaves off, but fits trendlines directly to the B1-#2,5 correlations revealed in Part I. These trendlines allow a maker to compute B1-mode frequencies given the plate mode 2 and 5 frequencies. They are entirely dependent on experimental data for 10 violins, a situation that will naturally evolve as more mode frequency data become available.

EXPERIMENTAL DATABASE

We will be guided by experimental data on top and back plate modes as well as modal analysis or other well-defined ways of determining the corpus mode identity. We have two important data sets to analyze to develop relationships between plate modes and corpus B1 modes:

1. Schleske [6] in 1996 published the results of a systematic experiment on one unvarnished violin with neck-fingerboard, taking the top and back plates from initially very thick to final thicknesses in steps, at each step gluing the plates to the ribs and determining specific plate and corpus mode frequencies. For example, the top plate started at 88 g without bassbar, and ended at 67 g with a bassbar, while the back plate started at 168 g and ended at 111 g. For the top plate the steps also involved cutting *f*-holes and inserting the bassbar. Midway through the experiment the soundpost was inserted and the violin strung up.
2. VIOCADEAS[4] measurements on nine different violins with known modes 2 and 5 frequencies for the top and back plates [7], plus augmentation from more recent partial measurements on three Old Italian violins and two modern violins by well-known makers.

Schleske's experiment stands out for a number of reasons. One was the broad range, highly systematic approach uncommon for violinmakers. Another was that there was almost no dependence of B1 frequencies on plate mode frequencies. Hence, Schleske concluded that plate tuning to specific frequencies hardly seemed worth the trouble if the rationale for doing so was to reach certain "target" corpus mode frequencies. Given this conclusion, how are we to address the regularity seen in the Old Italian results of Fig. 1?

It is a reality that resonant frequencies depend on two basic parameters: stiffness and mass. In this context Schleske's experiment was one in which the major mass components of the corpus, the top and back plate, had their stiffness and mass changed significantly, but the assembled violin showed only minor corpus mode frequency changes. Why? It is reminiscent of the Sherlock Holmes case in which the dog did not bark. In short, the ribs were neglected. For example, adding the bassbar raised mode 5 from 308 to 373 Hz, a 21% increase, while $B1^-$ at 408 Hz moved up 1% and $B1^+$ at 529 Hz went up 2%. Why would such a large change in top and/or back plate frequencies create such relatively small B1 changes? We believe that over such an extraordinary range of measurements the one thing kept constant—the ribs—are not just a significant component in the corpus-bending stiffness, but the dominant one. The problem is how to "prove" this.

ANALYSIS PRELIMINARIES

Floppy, broken up by blocks, curvy and reverse-curvy in shape, the ribs are a terrible mechanical system to characterize in isolation. To attempt to treat them like the plates, we approach the violin in a highly generalized way, applying only the most basic physical principles of vibrations. Our approach is as follows:

- Take a complex shape and "flatten" it. (Do violin plates act enough like flat plates to do this?);
- Sandwich the major corpus components, the plates, around the ribs;
- Treat the ribs as a plate;
- Compare the rib to plate stiffness, assuming both are flat plates;
- Create a flat plate sandwich model B1-ZOM to aid analysis;

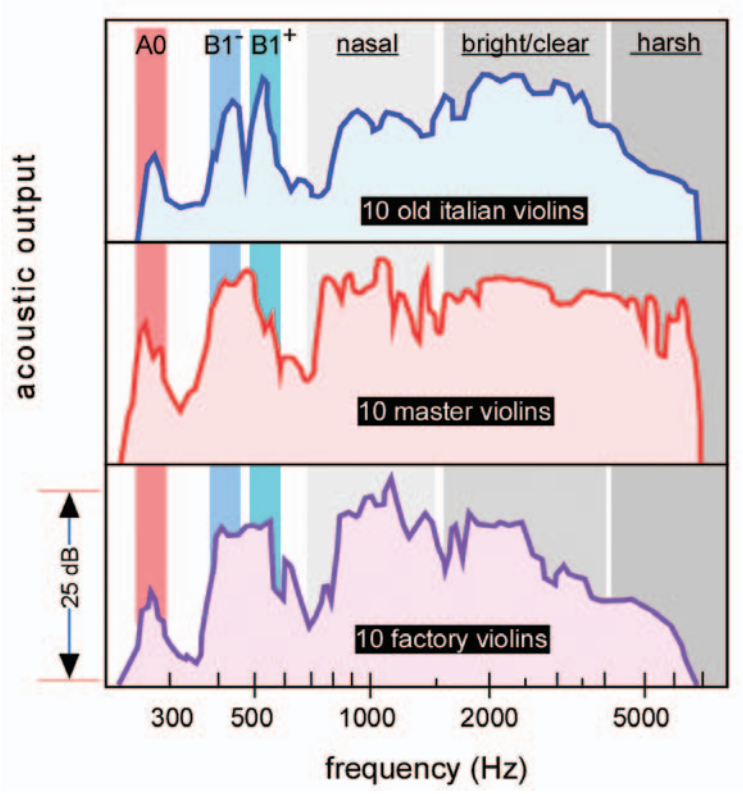

Figure 1. Envelopes for Dünnwald overlays of the acoustic output of 10 Old Italian, 10 master, and 10 factory violins up to ~7 kHz [5]. The major radiating signature modes, A0 (lowest cavity mode near 280 Hz) and the 1st corpus bending modes $B1^-$ and $B1^+$, are labeled. The regularity of the A0, $B1^-$, and $B1^+$ envelopes for the Old Italian violins is notable, but not for other classes.

- Allow the plates to bend in only one way along the ribs as suggested by modal analysis for the B1 modes (but not constrain plate motion away from rib line);
- Estimate plate-bending stiffness for each grain direction from the plate mode frequencies (tap tones) and plate mass;
- Estimate corpus stiffness from B1 mode frequencies and corpus mass (assume rib assembly mass = 50 g); and
- Estimate rib stiffness for each B1.

Does a Violin Plate Act Like a Flat Plate?

The first step in the process is to see how much a violin plate behaves like a flat plate, which has a frequency of vibration directly dependent on its thickness h (always much less than the length or width of the plate). This will show up as a straight-line behavior when frequency is plotted vs. thickness on a scatter plot.

Schleske's data for the back plate in successive thinning stages are a convenient starting point. The original plate thickness was 5 mm, uniformly graduated. Successive thinning stages were not necessarily uniform so it was assumed that the mean thickness could be computed from the plate mass m divided by the original plate mass of 168 g, or h(mm) = m/168 x 5 (back plate). Figure 1 shows a scatter plot of back plate mode frequencies vs. mean plate thickness h. Similar mean thickness relationships were used for the top plate, but the insertion of the bassbar makes this data sequence much different than for the back plate, since it is essentially broken into two sequences. The plot of the top plate data is also shown in Fig. 2 and the pre- and post-bassbar points are differentiated.

Of course, violin plates are really three-dimensional "shells."[5] This means that if you push straight down on a plate lying on a table, the plate edges extend outward. This horizontal motion reflects the additional *extensional* character of shell vibrations that comes right along with the flexural behavior characteristic of flat plates. It is important to note that the flexural behavior of a surface is what produces sound; extensional motion can only end up as heat.

How do we determine whether extensional or flexural shell behavior predominates in a violin plate? The short answer is to thin it in stages and plot the mode frequency vs. mean thickness

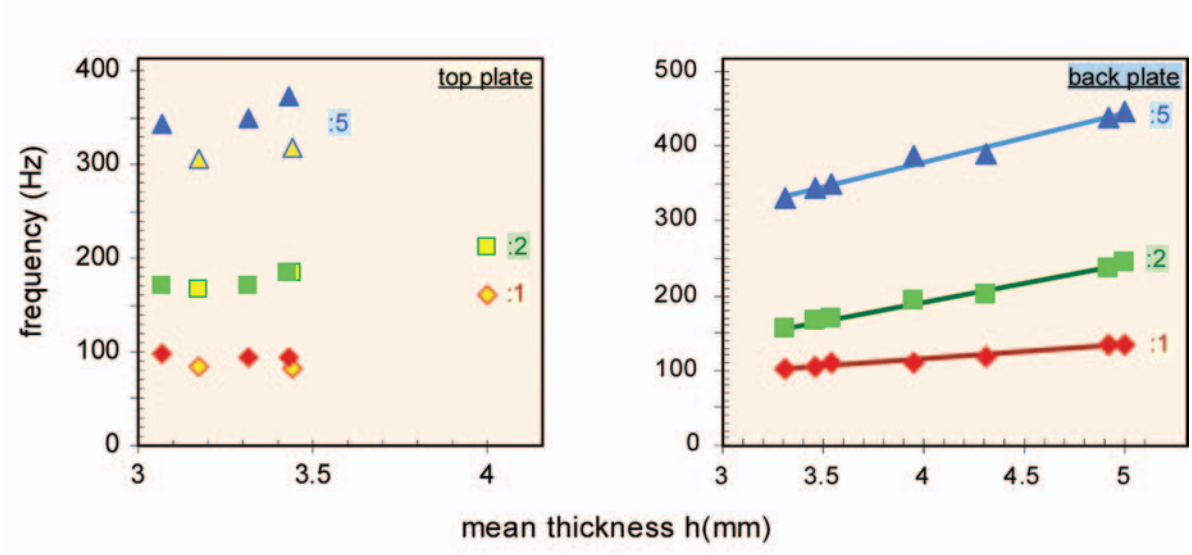

Figure 2. Scatter plot of mode 1, 2, and 5 frequencies vs. plate mean thickness (Schleske data [6]) for top (left) and back (right) plates. In the top plate figure pre-bassbar points are shown with yellow fill color (mean thickness with bassbar-in computed from overall mass). The data patterns for back plate modes 1, 2, and 5 look like straight lines, so linear trendlines were computed and are shown superimposed on the data (all r > 0.98, indicating good reliability). Note that the frequency differences between modes 2 and 5 also follow a linear trend (but top plate data must be separated into pre- and post-bassbar sets).

in a scatter plot, just as in Fig. 2. If the straight-line fit equation gives a zero intercept (anything within ±10 Hz is "zero") when h = 0, the mode is primarily flexural in character. On the other hand, if the intercept frequency is more than 20-30% of the mode frequency there is a significant extensional component along with the flexural. As an example, using the straight-line fits in Fig. 2 (back plate only) for mode 2, f = 49.9·h - 7.7, while for mode 5, f = 65.0·h + 119. Since mode 2 has essentially a zero (7.7 Hz) intercept, it is primarily a flexural mode, while for mode 5 the intercept is 119 Hz—36% of the mode 5 frequency—and there is clearly lots of extensional behavior in this plate mode.

The top plate, with *f*-holes cut out and bassbar inserted, is more complex, but it shows similar trends pre- or post-bassbar.) Note that the mean thickness with bassbar-in was computed from overall *mass*, a practical and reasonably plausible way to take the bassbar into account.) However, the bassbar clearly affects mode 5 much more than mode 2, as expected, since this mode flexes the plate across the grain. Mode 2 flexes the plate along the grain, in a direction perpendicular to that for mode 5, and thus is relatively unaffected by the bassbar. For our purposes, violin plates seem sufficiently flat-plate-like to apply some highly simplified mechanical modeling. We next address arching effects in the context of achieving certain mode frequencies.

Does the Arching Make Any Difference?

If all we care about are plate mode frequencies, then arching is not important. There is ample range to thin plates to achieve a traditional frequency. If we care about mode shapes, then there is empirical evidence from the experiment that we discuss below to answer this question. If we want to know how arching affects violin tone and the way a violin radiates sound, then the answer is that we know it does, but we will not address that matter here.

Suppose archings were changed from low to high and curved to flat. Would this affect our flat plate assumption? This question has been reduced here to: Would the arching affect the mode shapes that we will use in relating free plate modes to assembled instrument modes? A 30-year-old series of experiments on bassbar tuning in plates with widely varying arching provided a check on how arching affects mode shape and frequency data [8]. Pictures of modes 2 and 5 for 10 different plates were so similar that it was impossible to relate a Chladni pattern to the arch. (Five photo examples of each of these modes are shown in Fig. 3, along with a cross section of various archings employed for specific plates.) Based on these experimental results we are going to assume plate arching is *not* an important consideration in whether modes 2 and 5 will appear at any particular frequencies, or whether they can be treated as approximately flat-plate bending modes.

THE B1 ZEROTH-ORDER MODEL

Schleske had concluded from his experiment that plate tuning hardly affected corpus signature mode frequencies, and hence the rationale behind free plate tuning was questionable. Of course, his data *do* show that thicker plates give higher corpus mode frequencies—as they must—just that corpus frequency changes seem much diluted. It is a basic tenet of modal analysis that substructures assembled into structures carry their mode parameters into the whole in some form, adding modes to the conglomerated structure and thereby increasing the overall mode density (= #modes/frequency interval) of the structure. Since plates are the major substructures in the violin corpus, and plate modes 2 and 5 are among the lowest frequency ones, we would expect the strongest relationships to be with the lowest corpus modes.

The ribs are tough to handle since their mechanical stiffness properties—thin and floppy in isolation, with blocks of various shapes interrupting the ribs—change so dramatically when glued to the plates. What is clear, however, is that bending the plates *must* bend the ribs (any shear effects will be neglected completely). Since ribs are also quite high relative to plate thickness, and we know that in a plate the stiffness will vary as thickness cubed, we have reason to believe that ribs, in addition to their cavity-forming duty, can contribute significantly to the corpus stiffness. Of course, since the ribs are glued to the plates their stiffness must, to some extent, depend on the plate stiffness, but this complication will be

addressed when we reach it.

At this point, we attempt to make this hand-waving a bit more formal *for the 1st corpus bending modes only*, in what we will refer to as the B1 zeroth-order-model or B1-ZOM for short. In physics, a first-order model implies neglecting a lot of details, which will then be treated in a higher-order model. In the B1-ZOM details are trashed immediately with no hope of reclaiming them later, e.g., ribs = flat plate, no arching, no corpus modes but $B1^-$ and $B1^+$, no plate modes but 2 and 5, no distinction between boundary conditions (free-free for plate modes and presumably simply-supported for the same plates in the corpus modes $B1^-$ and $B1^+$). Such enormous simplifications provide us with a mainly conceptual model that sometimes suggests an experimental test as in Fig. 2. Usually we will have to be satisfied with statistically significant correlations between one parameter and another, which is where the scatter plots will come in. In short, this B1-ZOM is a heuristic model based on plausible arguments that we hope can be supported by results; it is *not* to be confused with a real physics model of the violin.

Plain Geometry

To set the stage for the B1-ZOM, we refer back to typical nodal line patterns for modes 2 and 5 in the top plate in Fig. 3. These plates had very widely varying archings but similar nodal line patterns, indicating that arching does not change the basic patterns. With these shapes in mind, look at the measured corpus bending modes shown in Fig. 3 compared with the free plate modes 2 and 5 in Fig. 3. The side-view modal analysis results for the B1 mode ribs, compared to side-view results for free top and back plates mode 5, show unmistakable common bending behavior along the rib line. That same bending behavior can be seen for mode 2 (back plate only), also shown in Fig. 4.

The geometries in Fig. 4 suggest treating the violin corpus as a dynamic wood sandwich where top and back plates act as bread to the ribs' meat, leading directly to the B1-ZOM sandwich version of the violin corpus. Corpus modal data with the top and back plate nodal lines, as shown in Fig. 5, were metamorphosed into a flat-plate version where the top, ribs, and back are all sandwiched plates required to bend from the rib side as shown in Fig. 4. Note that this condition does *not* force the center of the plates to bend the way the ribs do.

B1-ZOM Corpus Stiffness

A schematic version of Fig. 5 is shown in Fig. 6, where the plate sandwich was used to create a mass-spring analog good only for the B1 modes. Since a mass-spring system has a frequency computed from $f = (K/M)^{1/2}/2\pi$, the measured plate frequencies and masses were used to make a crude estimate of the individual plate stiffnesses. The overall stiffness (just B1 modes!) is the sum

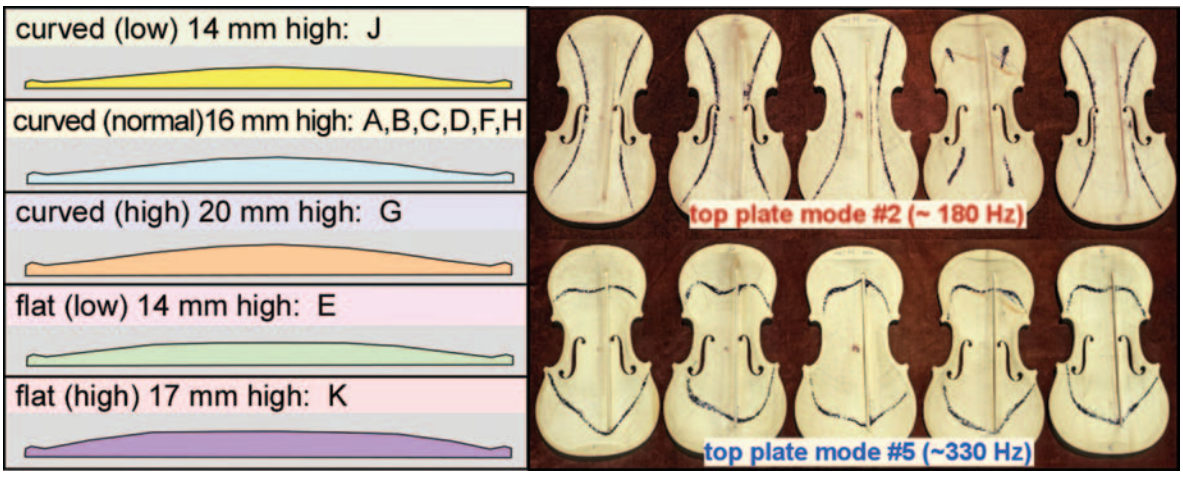

Figure 3. Five (out of 10) individual plate Chladni-pattern nodal line patterns for mode 2 (top right: nominally 180 Hz) and mode 5 (bottom right: nominally 330 Hz) for a wide range of arching (left) from low curved to high flat.

of the top, rib, and back stiffnesses: $K = K_T + K_R + K_B$. Similarly, the corpus mass $M = m_T + m_R + m_B$. Furthermore, since Fig. 5 shows different top and back plate flexures for each B1 mode, the respective top and back plate stiffnesses must reflect this detail.

No rib mechanical property information was gathered in the VIOCADEAS measurements except for the CT scans, which did not have sufficient resolution (pixel dimensions = 0.6 mm) to really get accurate thickness or density from perpendicular slices. (Analysis of diagonal views has not been done at this stage.) Other than not being too thick or thin, with the curl matching that of the back plate, ~29-31 mm high, etc., the working characteristics of maple ribs seem to be based mostly on appearance. Hence, a "rib" mass was taken for a "typical" violin as nominally 50 g, with ~30+% from the ribs proper. This total value was used for all the Schleske and VIOCADEAS data analysis. Since different makers make different choices for those subsidiary parts that make up the "ribs," it is probably safe to assume that the so-called rib mass—and computed stiffness—will vary from maker to maker. Building rib assemblies in a consistent way is a good way to understand systematic trends.

If the rib stiffness were actually larger than the top and back plate stiffnesses together, then the insensitivity of the B1 modes to plate thickness changes is a straightforward consequence of the usual equation relating mass and stiffness to resonance frequency. To estimate rib stiffness we exploit the geometry shown in Fig. 5. $B1^-$ was assumed to have the top plate motion looking like plate mode 2 and the back like mode 5, while $B1^+$ has the top motion like mode 5 and the back like mode 2. These bending geometries suggest specific stiffnesses for the sandwich components: as an example, for $B1^-$ $f_{T2} = (K_{T2}/m_T)^{1/2}/2\pi$ was used to estimate K_{T2} from mode 2 for the top. Similarly, K_{B5} was computed from mode 5 frequency for the back and K- from the corpus $B1^-$ frequency and corpus mass; for $B1^+$ K_{T5} was estimated from mode 5 for the top and K_{B2} from mode 2 for the back and K+ for the corpus from $B1^+$. In both cases the rib stiffness was estimated from $K_R = K - K_B - K_T$. Rib stiffness results from this B1-ZOM analysis for steps 4c to final step 14f are shown in Fig. 7, along with plate stiffness estimates for comparison. A logarithmic plot was used to see plate stiffness *variations* on the same scale as the rib stiffness variations.

Figure 7 gives some insights into the relative stiffnesses of the various corpus components and their evolution as the plates are thinned. Note that top plate stiffness is not as large as back plate stiffness due to the plate *mass* difference, not to the mode 5 frequency difference. Rib stiffness exceeds individual plate stiffnesses from step 6c onward, culminating at step 14f with rib stiffness considerably larger than the *sum* of

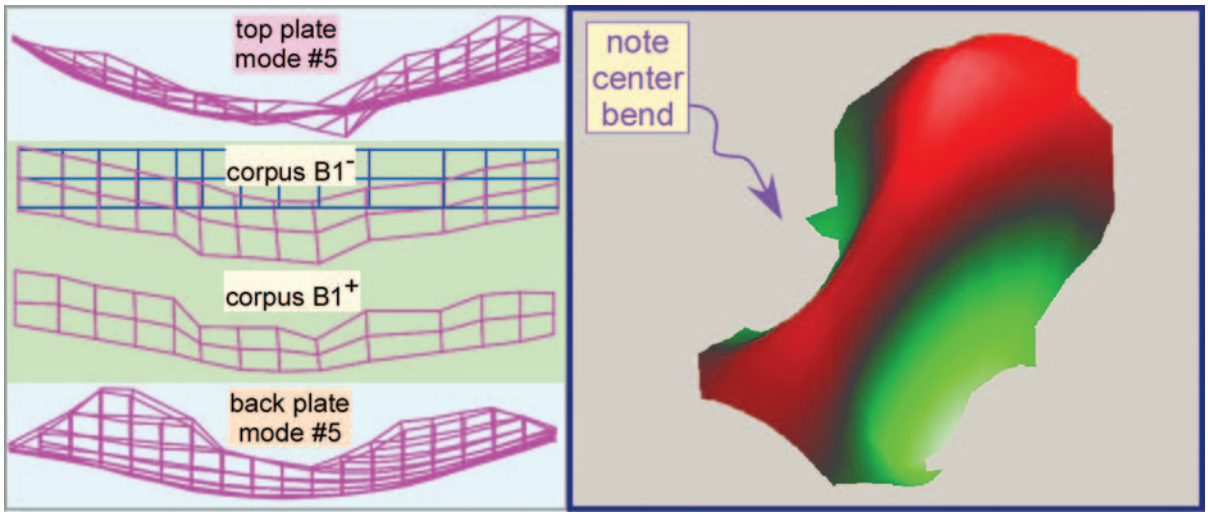

Figure 4. Left: Experimental modal analysis results for the B1 modes showing side view of rib bending as well as mode 5 for top and back plates. Right: Back plate mode 2 showing bending in the C-bout region similar to mode 5.

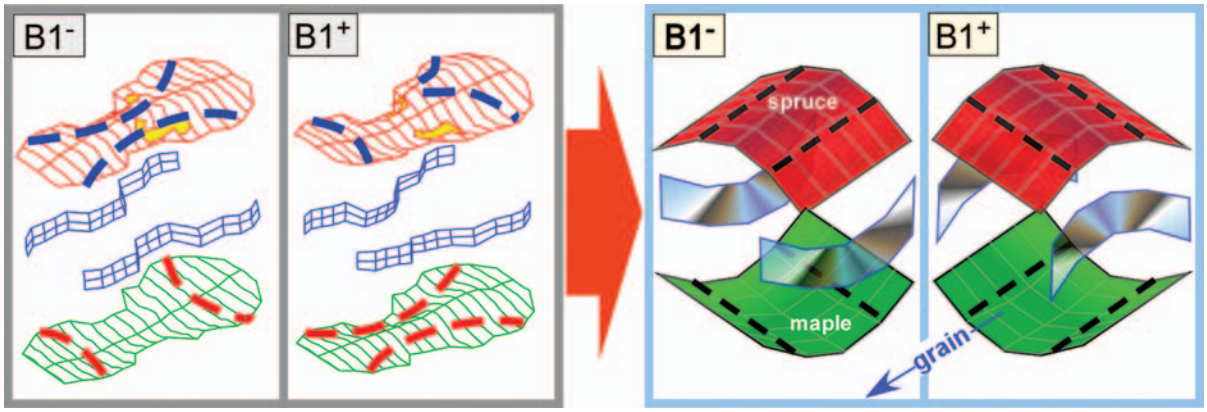

Figure 5. Left: Violin modal analysis results for B1⁻ and B1⁺ showing top, ribs, and back (nodal lines superimposed on top and back). The nodal patterns are strikingly suggestive of modes 2 and 5 in the free plates (especially for the top plate, the back mode 2 is often more like two "V"s inverted at either end); Right: B1-ZOM flat plate sandwich analog.

plate stiffnesses. The effect of thinning the back plate on rib stiffness estimates is somewhat easier to follow since it did not have the complication of bassbar insertion. Going from step 9f to 14f (*after* bassbar, soundpost insertion, stringing-up), estimates of K_{R-} changed by <1%, while K_{R+} dropped by 16%. For B1⁻, compare this to a 25% drop for the top plate K_{T-} and 39% for the back K_{B-}, while for B1⁺, the top K_{T+} dropped by 24% and the back K_{B+} by 46%. A plausible explanation for the difference is the much smaller top plate stiffness for in-out rib motions on the side of the violin. Although these stiffness estimates are quite crude, they are consistent throughout the steps, arguing for both K_{R-} and K_{R+} being nominally constant after the instrument was strung up (steps 9f-14f) in support of a basic assumption that rib stiffness did not change during this experiment. Of course, gluing ribs to plates means that plate stiffness must in some way affect rib stiffness (and conversely).

Are the Ribs Really that Stiff?

Figure 7 clearly shows that rib stiffness domi-

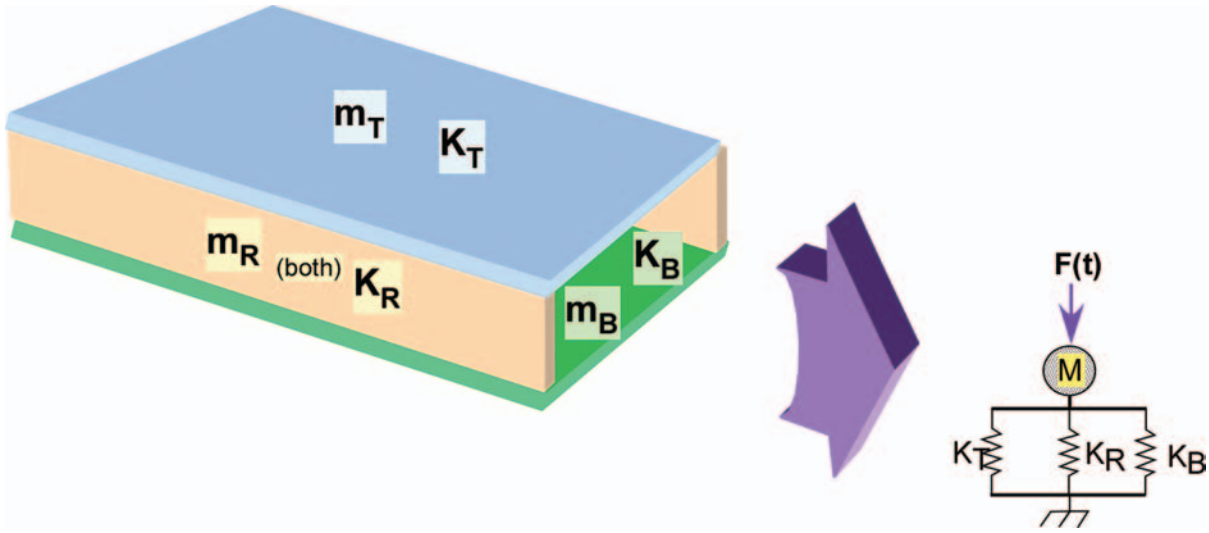

Figure 6. B1-ZOM corpus sandwich model and its corresponding mass-spring analog for the B1 modes.

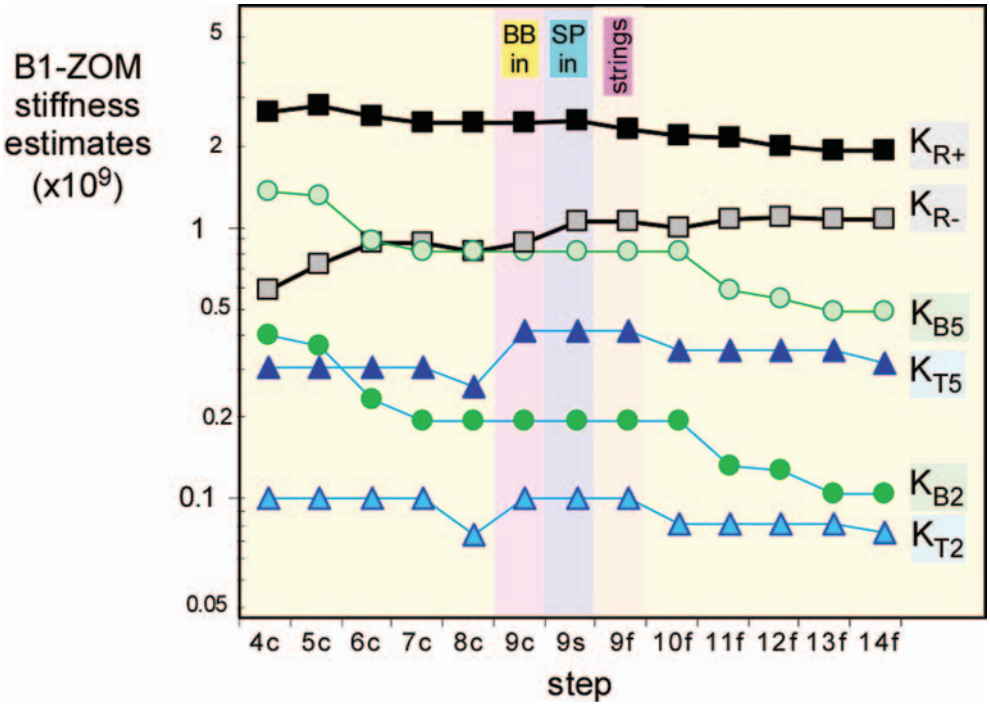

Figure 7. Logarithmic plot of B1-ZOM stiffness estimates for top and back plates K_T and K_B, and ribs K_R for B1⁻ and B1⁺ as violin plates were stepped through various plate-thinning steps, plus bassbar, soundpost insertion, and stringing up operations, in Schleske's experiment [6].

nates overall corpus stiffness. Is this reasonable? An independent check on this result comes from simple flat-plate equations. If a flat plate is loaded at the center by a force F and bends an amount x, its stiffness $k = Ewh^3/DL^3$, where E is Young's modulus, w is the plate width, h is the thickness, L is the length, and D depends on where the force is applied. Choosing nominal values for these parameters (plate bent perpendicular to plane, ribs bent in-plane),

- Plates: h = 3 mm, w = 200 mm, L = 350 mm,
- Ribs: h = 30 mm, w = 1 mm, L = 350 mm (the ribs are rotated 90°),

and assuming the same materials throughout so that E is the same for all, the ratio of rib to plate stiffness cancels out E, D, and L. Thus, we end up with a ratio $k_{ribs}/k_{plates} \approx 5$. This is quite near the ratio from Fig. 7 when the top and back plate stiffnesses are averaged. This simple calculation, in which the cube of the 30:3 thickness ratio overcomes the 200:1 width ratio, supports the contention that the ribs are really dominant in bending mode stiffness. Of course, our assumption that the ribs bend in-plane is reasonably close to what we observe—but not exactly.

What the Ribs Do

VIOCADEAS modal analysis animations generally showed that rib motions at the top plate for B1⁻ were larger than at the back plate, while the opposite was true for B1⁺. They also showed that the ribs toed in on the top plate and out on the back for B1⁻, while reversing this behavior for B1⁺, consistent with the plate modes switching. This means that the assumption of the ribs bending in-plane is only approximately true.

An interesting effect (not yet understood) was the difference in rib stiffness trends, with K_{R-} increasing until step 9s (soundpost inserted), after which it remained the same, while K_{R+} generally decreased overall, dropping 25% from step 1c to step 14f. Both rib stiffnesses showed an increase when the soundpost was inserted, presumably reflecting increased corpus stiffness

from coupling of the top and back plates. The soundpost-stiffening effect is readily seen in the frequency rise of A0 when the soundpost is inserted, due to cavity wall stiffness increasing, and also in small, generally upward corpus mode frequency shifts [9].

Similar stiffness analysis was applied to three VIOCADEAS violins with known plate mass and mode 2 and 5 frequencies. These rib stiffness estimates are shown in Fig. 8, which is a plot of estimated rib stiffness vs. top and back plate stiffness for $B1^-$ and $B1^+$. Also included are the Schleske data from Fig. 7 to compare the effect of plate thinning on one violin's rib stiffness with final violin results. Figure 8 shows again that $B1^+$ rib stiffness is more sensitive to back and top plate stiffness variations than $B1^-$. Note also that stiffness of the top is much less than that of the back for $B1^-$, whereas for $B1^+$ they are much closer, as expected from the basic grain-direction-dependent spruce and maple stiffness properties (see Fig. 5). Not surprising, there is good agreement between both data sets, although individual maker's choice of woods and construction techniques can cause significant differences in the rib stiffness.

These estimates of the plate and rib stiffnesses indicate that the finished violin has most of the overall corpus stiffness in the ribs for both B1 modes: more than 60% for $B1^-$; >80% for $B1^+$. Overall, high rib stiffness explains the insensitivity of the B1 modes to changes in the plate mode frequency because rib stiffness dominates the overall stiffness in the equation for resonance frequency. Rib stiffness should dominate corpus stiffness in violins with traditional construction. If the estimates of rib stiffness had been very close among all four violins, we could argue that rib stiffness be considered constant and set equal to the average for each B1 mode. Figure 8 argues they are not constant, although they are fairly close to one another. Since rib stiffness dominates corpus stiffness, and it varies from violin to violin, applying the B1-ZOM model directly to a

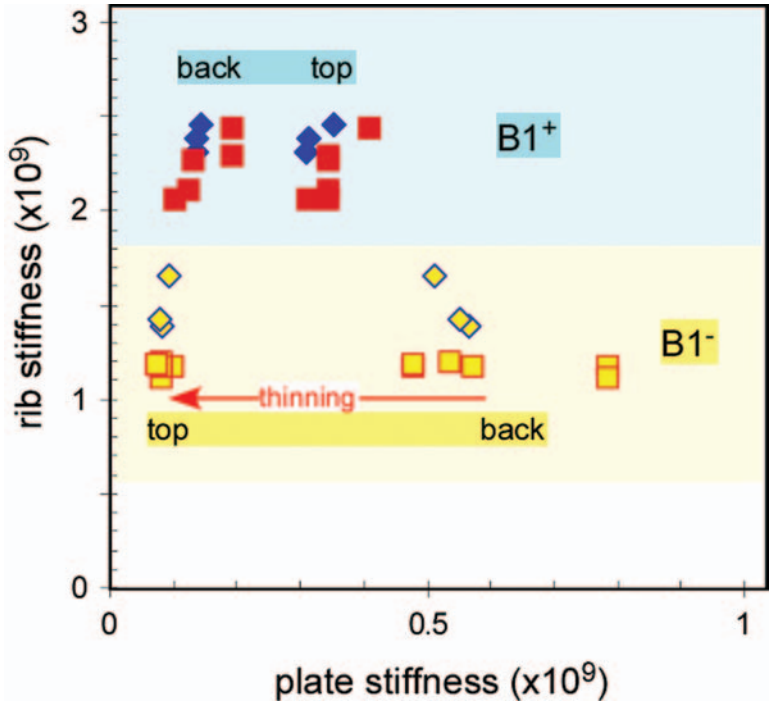

Figure 8. B1-ZOM estimates of rib stiffness (assuming rib mass = 50 g) vs. top and back stiffness (see plate notations) for $B1^-$ (lower region) and $B1^+$ (upper region): 1) for three VIOCADEAS violins with known plate masses and mode frequencies ($B1^-$: ◇; $B1^+$: ◆), and 2) Schleske's sequential results from steps 9f-14f after f-holes, bassbar, soundpost and stringing up ($B1^-$: □, $B1^+$: ■). Rib stiffness was insensitive to plate thinning for $B1^-$, whereas $B1^+$ rib stiffness dropped ~16%. VIOCADEAS $B1^-$ results were slightly higher and scattered and showed opposite trends between top and back, whereas $B1^+$ rib stiffness trends were similar to Schleske's results [6].

violin with rib stiffness assumed as constant does not seem useful.

At this stage it is clear that we must adopt an alternate strategy to develop a reasonably clear logical path from plate mode frequencies to B1-mode frequencies. The first step follows the B1-ZOM path a little further to see what we can mine from it. The second is to look directly at all of our plate and corpus data, and to work on trendlines extracted from fits to the actual data, possibly guided by the B1-ZOM (to be included in Part II).

B1-ZOM and Plate Modes 2 and 5

Schleske's data provide an insight into rib stiffness that the more usual whole-violin–free-plate vibration measurements cannot. Yet the same basic physical mechanisms still hold for any playable violin. Consider the heuristic B1-ZOM equations with specific contributing modes 2 and 5 plate stiffnesses for $B1^-$ and $B1^+$: $K_{B1-} = K_{T2}+K_{B5}+K_{R-}$; $K_{B1+} = K_{T5}+K_{B2}+K_{R+}$. If we compute the frequency difference $\Delta B1 = B1^+ - B1^-$,

$$\Delta B1 = (1/2\pi)\{[(K_{T5}+K_{B2}+K_{R+})/M]^{1/2} - [(K_{T2}+K_{B5}+K_{R-})/M]^{1/2}\}. \quad (1)$$

We assume that K_R is approximately the same for each B1 (actual 4-violin average: $K_{B1+}/K_{B1-} = 1.6\pm0.3$) and that K_R is much greater than $K_T + K_B$ (not really true for $B1^-$, but necessary to do some simplifying math). Then we can write (we drop some numbers like 2π after manipulation for convenience and use the "varies as" symbol $\propto$),

$$\Delta B1 \propto (1/K_R M)^{1/2} [\,(K_{T5} - K_{T2}) - (K_{B5} - K_{B2})\,]. \quad (2)$$

Equation (1) suggests that ΔB1 depends primarily on the rib stiffness, so that if the plates become very thin and rib stiffness truly dominates corpus stiffness, ΔB1 approaches a constant value given by $\Delta B1 \approx [(K_{R+} - K_{R-})/M]^{1/2}/2\pi$. Equation 2 suggests that ΔB1 depends in some way on mode 5–mode 2 stiffness *differences*. If these go to zero, so does ΔB1, but this is possible only if plate thicknesses go to zero (see Fig. 2) or if $K_{T5} - K_{T2} = K_{B5} - K_{B2}$. (Here is where reality intrudes somewhat. K_R cannot be the same for the two B1 modes. If it were, $B1^+$ would be the lower frequency mode because the term inside square brackets [ ] in Eq. (2) would be negative! See Fig. 7.)

Schleske had clearly shown that B1-mode frequencies were not very sensitive to the plate mode frequencies themselves, and we have seen that dominant rib stiffnesses in the B1-ZOM can explain this insensitivity. However, taking B1 corpus mode frequency *differences* points toward possibly a better way to understand how plate modes 2 and 5 really affect these mode frequencies, as suggested by Eq. (2). ΔB1 will now be treated as if it were sensitive in some way to *differences* between mode 5 and mode 2 frequencies in the top and back plates! Procedural hints from these equations led to what seemed to be a million "scatter" plots—mercifully glossed over here—before finally finding one showing a meaningful correlation between modes 2 and 5 and the B1 modes. (The whole procedure was quite mindful of what J.R. Oppenheimer [10] described as the "bumpy contingent nature of the way in which you actually find out something" in science.)

The obvious scatter plot of ΔB1 vs. Δ5-2 for Schleske's data showed *no* significant correlation (Δ5-2 is just the average difference between the free-plate mode 5 and mode 2 frequencies—obviously no rib effects here). However, a strong correlation was found between the ratio ΔB1/Δ5-2 vs. ΔB1 (but not vs. Δ5-2) as shown in Fig. 9. This scatter plot covers the entire Schleske experiment, including cutting *f*-holes, inserting the bassbar and soundpost, and stringing up the instrument. Figure 9 indicates that from step 1 before the *f*-holes are cut in the top plate up to the bassbar insertion step (step 9) there hardly seems to be a discernible pattern. But after insertion of the bassbar, soundpost, and stringing up the violin, the scatter plot also shows that the data points from steps 4 to 14 form a much more regular pattern if steps 1 to 3 are neglected.

We consider any regularity in quantitative analysis of violin data to be "interesting." Will the regularity seen for plate thinning (steps 9 to 14) in Fig. 9 also be seen for the nine different violins in the VIOCADEAS data where plate and corpus mode frequencies also were known? Figure 10 shows such a scatter plot with the VIOCADEAS data inserted. Remarkably, the data for the nine separate violins share the same regularity in ΔB1/Δ5-2 vs. ΔB1 as for one violin

undergoing extensive plate thinning.

Two 2nd-order polynomials were chosen as trendlines because a slight bend was seen in the pattern, one constrained to go through zero when ΔB1 = 0, and the other one not. A straight line was also a plausible choice here in terms of trends, but if the straight-line intercept were zero or very close, then the slope m = constant ≈ 1/Δ5-2. However, the experimental Δ5-2 data ranged from 159 to 203 Hz, hardly constant. There were also mathematical complications arising from solving simultaneous equations (using a later trendline equation for the frequency ratio of the B1 modes) that gave non-physical results, so it was dropped. The two 2nd-order polynomial trendline fits through all the data are shown in Fig. 10. The large correlation coefficient r = 0.95 indicates a reliable trendline.

It was surprising to find any strong relationship between plate and corpus mode parameters even for the few modes we have worked with. Quantitative relationships, such as suggested by the pattern seen in Fig. 10, are really quite scarce. Often in retrospect some are not what they originally seemed, e.g., the violin octet scaling procedure of Schelleng (which completely neglected the ribs!) used a nominal factor of 1.5x to scale the top-back plate tap tone (mode 5) frequencies to the "main wood" frequency. The Schleske data show this ratio starting at 1.23 and increasing to 1.37—an 11% increase—from steps 4 to 14, and that plate mode frequencies themselves seemed little related to corpus mode frequencies. Given the insensitivity of the B1 modes to plate tunings, this 1.5x factor seems somewhat fortuitous. Schelleng did not mention this factor in his scaling paper [3] nor did Hutchins in her violin octet history paper [4] or any other paper. The sole exception is a one-sentence remark in a 1967 *Physics Today* magazine article by Hutchins [11] about the main body resonance of a completed violin being approximately seven semitones above the main free-plate resonances. Other than Schleske's research, no other research addressing this relationship was found. Of course, if you are an

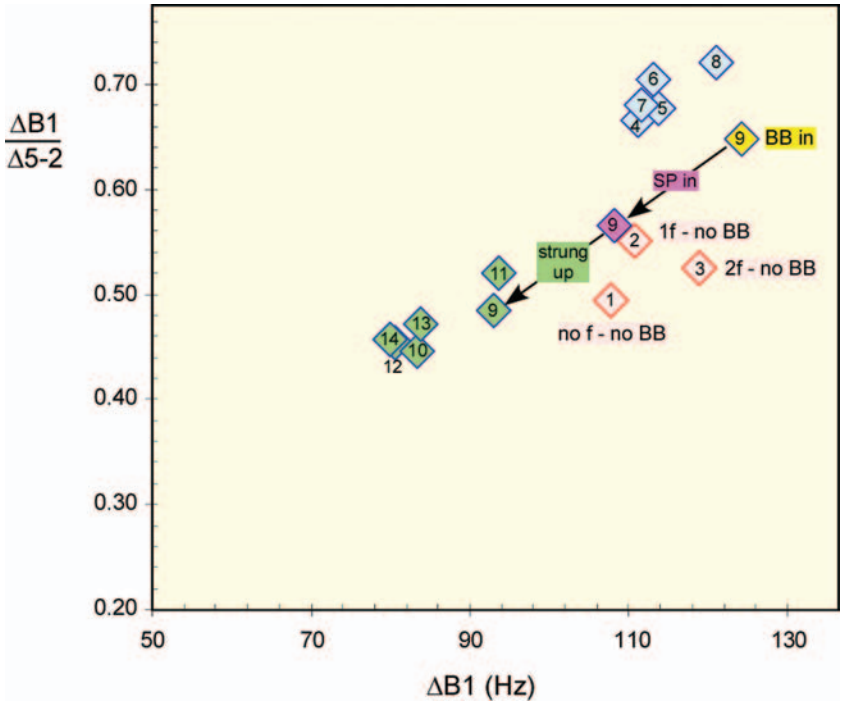

Figure 9. The ratio of frequency differences between the B1 modes ΔB1 and the plate modes 5 and 2 Δ5-2 vs. ΔB1 (Schleske's data steps 1c to 14f [6]). Steps 1-3 indicate earliest stages (no top plate mode 5 seen), steps 4-8 are for plate thinning, step 9 covers bassbar-in to soundpost-in to strung-up, then steps 10-14 again return to plate thinning. (Size of data points indicates approximate experimental errors in frequencies; internal numerals are step numbers.)

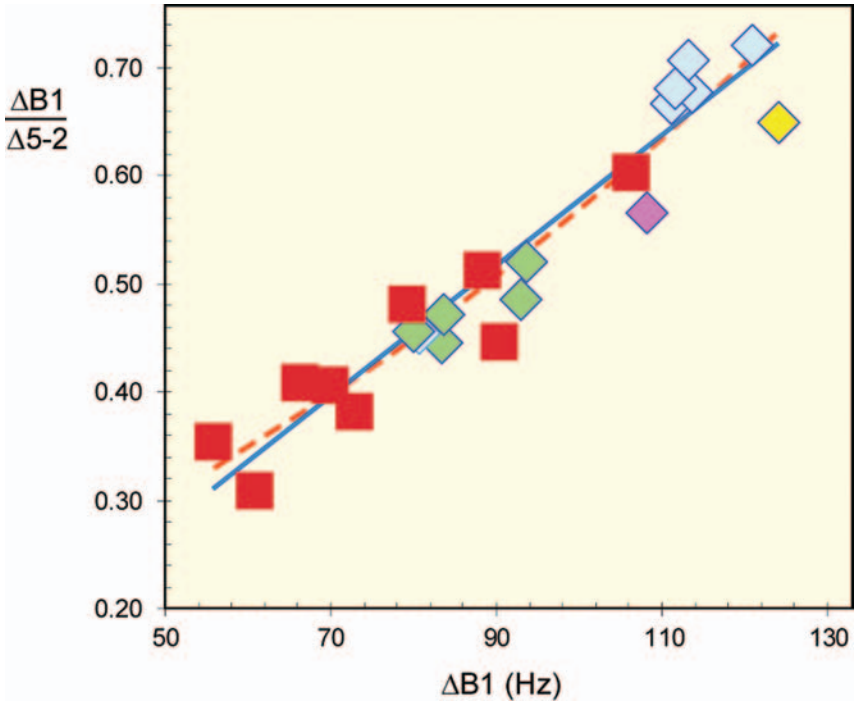

Figure 10. VIOCADEAS data for nine violins (red squares) added to Schleske's data [6] for one violin (steps 4-14 only). Two 2nd-order polynomial trendlines were applied to the data in a spreadsheet (both with correlation coefficient r = 0.95, indicative of a good fit) have been fit to this data: 1) $\Delta B1/\Delta 5\text{-}2 = 3.0527 \times 10^{-6}\ \Delta B1^2 + 5.3741 \times 10^{-3}\ \Delta B1$ (with equation constraint $\Delta B1/\Delta 5\text{-}2 = 0$ at $\Delta B1 = 0$; solid blue line), and 2) $\Delta B1/\Delta 5\text{-}2 = 2.0481 \times 10^{-5}\ \Delta B1^2 + 2.1249 \times 10^{-3}\ \Delta B1 + 0.145$ (orange dashed line). (Note that this regularity does not show up in a $\Delta B1/\Delta 5\text{-}2$ vs. $\Delta 5\text{-}2$ plot.)

optimist, how can you miss getting this ~1.5x factor if plate tunings do not strongly affect the final B1 frequency?

It is important to point out again that the regularity seen in Fig. 10 shows up for plate mode frequency *differences* only, presumably because generally the ribs so dilute the trends that the typical data scatter then buries real trends. This may be the first observation of a statistically strong relationship between plate and corpus mode frequencies. (But violinmakers, being somewhat secretive about what works for them, maybe just have not divulged such information.)

B1-ZOM—Another Equation

There is another crucial step required before we are able to start with plate mode frequency differences and end up getting B1 mode frequencies. We cannot get $B1^+$ and $B1^-$ from just the frequency difference; we need one more equation, i.e., two unknowns need two equations for solution. Returning to B1-ZOM, note that a ratio of $B1^+$ to $B1^-$ frequencies, R_{B1}, cancels out the total mass, a helpful simplification. Our equation then is just

$$R_{B1} = (K_{B1+}/K_{B1-})^{1/2} \qquad (3)$$

$$\approx 1.6^{1/2}\{1 + 0.5\,[(K_{T5} + K_{B2})/K_{R+} - (K_{T2} + K_{B5})/K_{R-}]\}, \qquad (4)$$

where Eq. (4) assumes rib stiffness is much greater than the sum of plate stiffnesses (good for $B1^+$ but not as good for $B1^-$). Again, if the B1 rib stiffnesses were approximately the same, we would end up with a $\Delta 5\text{-}2$ parameter in R_{B1}.

A positive frequency difference between the B1 modes obviously requires the frequency ratio R_{B1} to be >1. By the same token, no frequency difference means that the ratio must be exactly 1. The constraint $R_{B1} = 1$ at $\Delta B1 = 0$ was used in the polynomial fit to the experimental data.

Since we no longer require top and back plate mode frequencies, the data pool expanded to include 17 violins, including two by Stradivari and one by G. Guarneri *del Gesù*. Plotting R_{B1} vs. ΔB1 gives us the plot shown in Fig. 11. Here there can be no doubt of the link between the B1 frequency ratio and the frequency difference.

The data in Fig. 11 quite closely follow the polynomial trendline, although one point seems to deviate significantly more than the others. Closer investigation revealed that this particular instrument had an extraordinarily high bassbar for a violin formed after traditional patterns (see Fig. 11 inset). (It was from the University of Cambridge set of six violins built by David Rubio under the guidance of Jim Woodhouse [12]; modes 2 and 5 were matched at ~190 Hz and ~366 Hz respectively, in top and back plates, and mode 2 in the top plate was ~2X mode 1.) An extra-high bassbar will raise the mode 5 stiffness relative to mode 2, and since this mode 5 stiffness dominates the top plate motion for $B1^+$, while the back plate mode 5 stiffness dominates for $B1^-$, it perhaps is no surprise that the $B1^+/B1^-$ ratio is higher than usual. It seems reasonable to assume that trends seen in our violin data pool were *only* for the more traditional violins, with traditional dimensions for the various substructures, plates tuned in traditional ways, built with traditional materials and construction techniques, until proven otherwise. Non-traditional instruments need not apply—yet.

Getting B1 Mode Frequencies from Plate Mode Frequencies via Trendlines

Seemingly, Fig. 11 combined with Fig. 10 gives us all the information that we need. If we presume that the frequencies (and plate masses) of plate modes 2 and 5 are known, we can proceed from these frequencies via the two trendline equations to get estimates for $B1^-$ and $B1^+$:

1. the ΔB1/Δ5-2 equation relates Δ5-2 to ΔB1;
2. the R_{B1} equation relates ΔB1 to R_{B1};
3. $R_{B1} - 1 = \Delta B1/B1^-$;
4. so $B1^-$ can be linked to Δ5-2; and
5. $B1^+ = B1^- + \Delta B1$.

The simultaneous solution of our two trendline equations then allows us to plot predictions for $B1^-$, $B1^+$, and ΔB1 vs. Δ5-2 along with all the available experimental data in the scatter plot shown in Fig. 12. Clearly, these trendline equations, while giving ballpark values, are not very accurate representations of the experimental data. Such results just underscore our cautions about trendline equations not being based on fundamental physics. Rather, they are only statistical correlative equations guided by our heuristic approach. The choice of mathematical equation fit to the experimental data is somewhat arbitrary, and constraints generally help—the unconstrained Fig. 10 trendline (not used in Fig. 12) gave much poorer results. With a heuristic model there is no physics-based equation we can use with the data. However, the regularities shown in Figs. 10 and 11 still hold since they are based on actual data and not trendlines. Hence, the values read from each plot—noting the data spread for any one ΔB1, especially in Fig. 10—can be used to estimate the B1 mode frequencies and provide some reasonable estimate of the error accompanying the calculation of each.

How Does ΔB1 Change as B1 Mode Frequencies Increase?

First we will clean up some ambiguity in Figs. 10-12 directly. Does ΔB1 increase or decrease as B1 mode frequencies increase? From a plot of the Schleske data in the final strung-up stages (steps 9 to 14) plus the nine-violin VIOCADEAS data for ΔB1 and $B1^+$ vs. $B1^-$ frequencies in a scatter plot in Fig. 13, it is clear that ΔB1 generally *decreases* as the B1 frequencies increase.

Can B1-ZOM Eq. (1) help us understand this behavior? If we assume that rib stiffnesses are essentially constant although different, as plate thickness increases, the frequencies of modes 2 and 5 increase and B1 frequencies increase also. Thus, each term in Eq. (1) increases as expected. But using Fig. 7, while the rib stiffness $K_{R+} > K_{R-}$, the summed plate $B1^-$ stiffnesses $K_{T2} + K_{B5}$ is greater than that for $B1^+$, $K_{T5} + K_{B2}$. So, as plate thicknesses increase, the plate contribution in the second term grows faster than that in the first term, decreasing the *difference* between terms, and decreasing ΔB1. So yes, B1-ZOM does anticipate the trends seen.

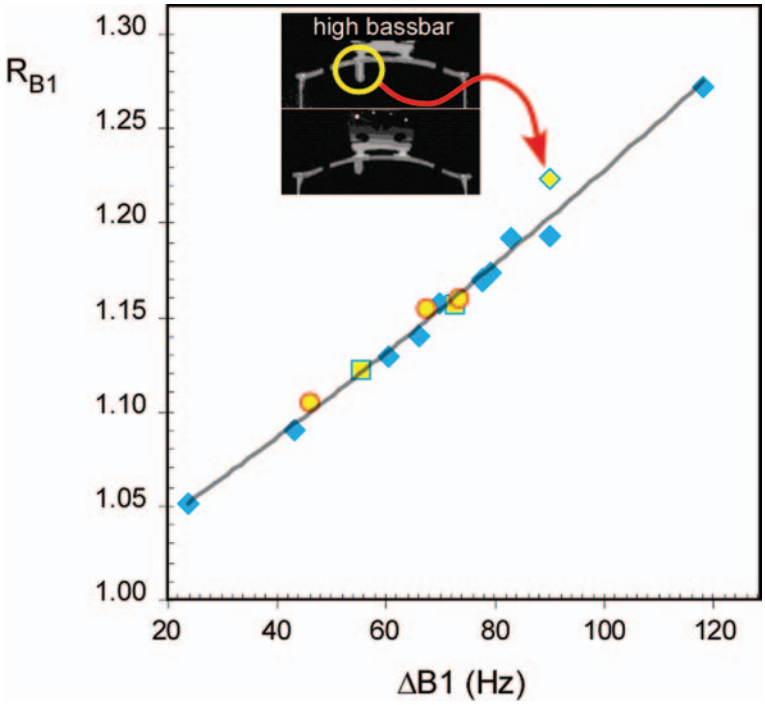

Figure 11. Ratio of B1 frequencies R_{B1} vs. the difference in B1 frequencies ΔB1 for finished, set-up violins. The 2nd-order polynomial frequency trendline was generated only for the constrained case where the intercept was fixed at 1: $R_{B1} = 3.129 \times 10^{-6} \cdot \Delta B1^2 + 1.927 \times 10^{-3} \cdot \Delta B1 + 1$ (r = 0.99). The plot includes two bent-wood (□) and three Old Italian violins (○). The one violin that deviated conspicuously from the trendline had an extraordinarily high bassbar (see CT scan insert with standard bassbar for comparison).

SUMMARY

The B1-ZOM equations and suggestive parametric dependences derived from them have culminated in a not very impressive linear trendline representation of the B1 data vs. Δ5-2. In Part II of this analysis we will work directly with the B1 data and Δ5-2 to attempt to take advantage of the observed significant correlations. However, it is important to summarize our progress at this point:

1. The Schleske experiment clearly showed that the long-term neglect of the ribs' important contribution to the overall vibrational properties of the violin was unwarranted. The fundamental reason that tuning plate modes to particular frequencies fails to ensure that B1 corpus mode frequencies will fall at particular places is the dominant role of the ribs in the bending mode stiffness.
2. While arching is important to violin radiation, all 17 violins tested to date show all the signature vibrational modes, irrespective of arching or quality.
3. Suggestive plate mode geometries led to a heuristic flat-plate-sandwich physical model of the violin—the B1-ZOM—to analyze frequencies of the 1st corpus bending modes and their dependence on plate and rib stiffness contributions. The B1-ZOM: a) provides estimates of rib stiffness compared to plates, b) predicts that thinning plates will have a progressively diminishing effect on B1 frequencies, in agreement with Schleske's experimental results, c) suggests that ΔB1 is related to Δ5-2, and d) guides us to why ΔB1 *decreases* as the B1 frequencies increase, in agreement with experiments.
4. Estimated rib stiffness depends to some extent on plate stiffness, primarily that of the back plate.

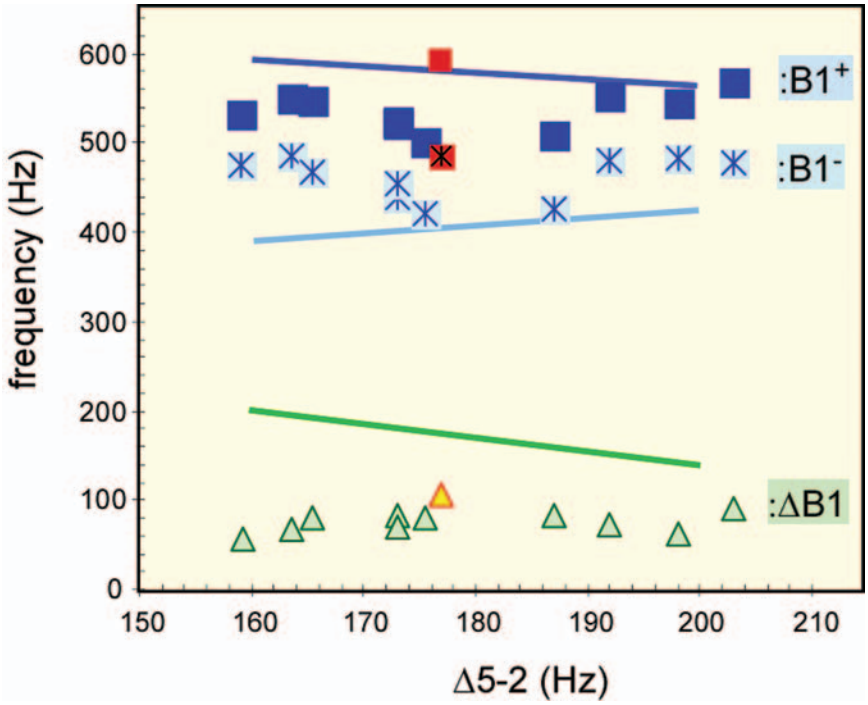

Figure 12. Trendline predictions for $B1^-$, $B1^+$ and ΔB1 vs. Δ5-2 along with nine VIOCADEAS and two Schleske [6] data points. The lines show simultaneous equation solutions from ΔB1/Δ5-2 (Fig. 11, constrained equation) and $B1^+/B1^-$ (Fig. 12) trendlines. The red-coded points are for the violin with an extra-high bassbar.

5. The ΔB1/Δ5-2 ratio shows an empirical regularity when plotted vs. ΔB1 for one assembled violin at various stages of plate thinning (after *f*-holes are cut), bassbar and soundpost insertion, and strings tuned, and this regularity holds for nine other finished violins.
6. After two centuries of scientific analysis of the violin, *any* quantitative relationship between violin substructures and the assembled structure is surprising and thus important.
7. The $B1^+/B1^-$ frequency ratio shows a strong dependence on ΔB1 and a reliable trendline, as expected.
8. Trendlines from ΔB1/Δ5-2 and $B1^+/B1^-$ vs. ΔB1, solved simultaneously, can be used to predict—although not very accurately due to trendline equation choice—$B1^-$, $B1^+$, and ΔB1 from the average difference Δ5-2 between the frequencies of plate modes 2 and 5.

REQUEST FOR DATA

Before publishing Part II, I would welcome emailed data sets (spreadsheet or organized text digital format) from willing makers that include plate mode 1, 2, and 5 frequencies and plate masses, as well as B1 mode frequencies (and any other signature mode frequencies measured reliably) and rib assembly masses (optional if you are close to 50 g). Individual maker's data would not be identified, but the maker would be acknowledged. When Part II is submitted to the *VSA Journal*, I would in turn provide an anonymous-pool spreadsheet for those who do submit data, including all data to that date, with some analysis and graphics included.

ACKNOWLEDGMENTS

The author wishes to acknowledge the support of the National Science Foundation in making the VIOCADEAS Project a reality, Tom King for information about rib masses, and Jim Woodhouse for the loan of the University of Cam-

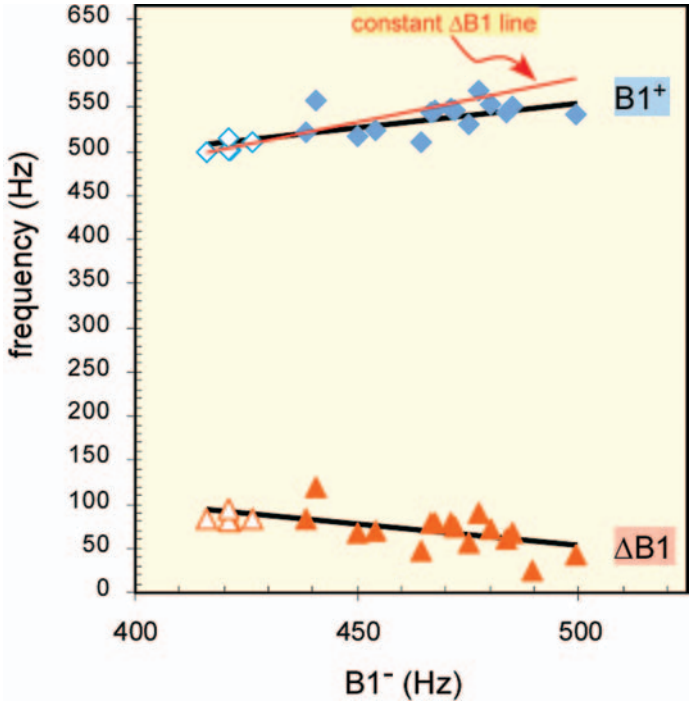

Figure 13. B1-mode frequency difference ΔB1 (lower data points) and $B1^+$ mode frequency (upper data points) vs. $B1^-$ frequency. Linear trendlines are shown for both data sets. (Filled points are VIOCADEAS data; unfilled points are Schleske data [6] for an unvarnished violin after f-holes, bassbar, soundpost, and stringing up.) Also shown for reference is a straight line representing $B1^+ = B1^- + 84$ Hz, i.e., a constant ΔB1 line (84 Hz from lowest B1 values) to make it more obvious that the spread in B1 frequencies is really decreasing slowly as $B1^-$ increases.

bridge collection of violins made by David Rubio and good discussions about violin physics, including the contents of this article.

NOTES

1. Modes: A brief clarification about modes vs. "normal" modes: A mode of vibration is a particular way an object has of vibrating. A certain shape (= motion profile) at a certain frequency is normally used to characterize a mode. We often consider a Chladni pattern of free-plate vibrations at a particular frequency as a convenient way to characterize mode shape, but it only defines the places where the plate has minimal (possibly zero) motion at a certain frequency. A "normal" mode shape is a bit—maybe a lot—different from a Chladni pattern, because it is the result of excluding the influence of all other modes during the analysis. *The "normal" label means that there is a certain mathematical operation performed, while creating each mode shape from experimental data, that renders each mode independent of all the other modes.* An analogy in a three-dimensional frame might be walking parallel to one wall in a rectangular room; this does not change your distance from that wall or the floor, just from the perpendicular wall. Perpendicular to the surface motion means "normal" to the surface in the usual mathematical terminology. Note that a finite-element simulation based on a solid model with reliable material stiffness and density properties with zero damping creates normal modes naturally because there is no response overlap that could intermix normal mode shapes at intermediate frequencies. These finite-element calculations should target individual experimental normal mode results to ensure that the material properties are reliable.

2. Scatter Plot: A scatter plot created in a spreadsheet is a very rapid and convenient way of determining relationships between parameters.

If parameter A is plotted vs. parameter B and an obvious pattern shows up in the scatter plot, it implies a relationship, whereas a point spray does not. Various trendlines (see Note 3)—straight, curved in many various ways as chosen from a menu—can then be fit to the data. The trendline will then be displayed along with the equation relating A to B and a correlation coefficient r indicating "goodness of fit," which ranges from 0, if there is no statistically significant relationship, to ~1, indicating essentially a perfect fit and very high statistical significance. In this article $r > 0.9$ will be considered strong evidence of a relationship. Note that the equation used for the trendline is suggested by the data pattern (eyeball choice), and *not* necessarily by any physics-type relationship!

3. Trendlines: It is convenient to summarize relationships indicated by these patterns in a mathematical form by fitting a trendline through the experimental data. Spreadsheet programs provide a menu of choices for the mathematical form of these trendlines, but here there is no clear physics guideline as to exactly what choice is best. Thus, a certain additional arbitrariness enters our heuristic model. In such cases, choosing very simple trendlines that don't "misbehave" just out of the range of fit seems appropriate. But this choice was *not* based on physics, just mathematical convenience. As a way of controlling possible mathematical misbehaviors it is sometimes possible to attach an additional condition that the fit equation must satisfy. In our case, we might require the ratio $\Delta B1/\Delta 5\text{-}2$ to go to zero as $\Delta B1$ goes to zero. Of course, this cannot be guaranteed, but it is certainly plausible unless the frequency difference between modes 2 and 5 went to zero also, requiring the highly unlikely scenario of plate thickness also going to zero. In fact, as noted above, B1-ZOM Eq. (1) indicates that $\Delta B1$ really can't go to zero because rib stiffness won't go to zero even if plate thickness goes to zero. (It is better not to ask how zero-thickness plates can be glued to the ribs, let alone hold them to shape.)

4. VIOCADEAS (VIOlin-Computer-Aided-Design-Engineering-Analysis-System—an acronym based on original IDEAS engineering software package) experiments involve: 1) measuring the violin's vibrations with a scanning laser system while tapping the bridge at the G-string corner with a small-force hammer, 2) simultaneous sound measurements over a sphere in an anechoic chamber, and 3) computed tomography (CT) scans of each violin to determine shape and density information about each violin. If the experimental measurements are combined with finite element calculations of violin vibrations based on a solid model created from the CT scans (with fixed shape and density properties), material stiffness properties can be extracted. If experimental top and back plate mode shapes and frequencies are available, it is possible to isolate the top or back plate in the computer model and calculate vibration mode frequencies and shapes for these separately, further improving our knowledge of the material properties of these two most important violin substructures.

5. Shells: For those interested in quantifying extensional vs. flexural, there is a generalized simple equation for a shell mode frequency $f = (A + Bh^2)^{1/2}$, where A and B are constant for a mode and only shell thickness h varies. This equation offers a guide to classifying whether a mode is primarily extensional or flexural. For example, a mode is primarily extensional if: 1) as h approaches 0, the mode frequency ≈ constant, or 2) $A >>> Bh^2$ so $f \approx$ constant again. A mode is primarily flexural if: 1) $Bh^2 >> A$, so $f \approx B^{1/2} h$, or 2) f vs. h plot looks like a straight line, *and* mode frequency is much larger than intercept (h = 0) frequency. While a spreadsheet generally does not allow you to use an arbitrary equation for trendline fits, this shell equation was used to compute frequencies with empirical choices for the A and B constants that achieved excellent agreement with the data in Fig. 2. The results for mode 2 were a frequency intercept of 0 Hz (this means $A^{1/2} = 0$ for h = 0) vs. typical mode 2 frequencies near 180 Hz; mode 5 had a frequency intercept of 220 Hz vs. a typical mode frequency near 330 Hz. From these numbers we can conclude that mode 2 is definitely flexural in character and that the plate behaves approximately as a flat plate. Mode 5, however, clearly has a lot of extensional character, although the thicker the plate, the less important this is. An interesting future simulation experiment would be to track mode frequencies vs. plate thickness for

varying plate archings—low, high, flat, etc. Beldie [13] has presented a very interesting photographic comparison of the evolution of flat, rectangular, spruce plate modes, to flat violin-shaped (with *f*-holes) plate modes, to arched violin top plate (with *f*-holes, but no bassbar) modes.

REFERENCES

[1] J. Schelleng, On vibrational patterns in fiddle plates, *Catgut Acoust. Soc. Newsl.*, No. 9, pp. 4-10 (1968).

[2] C.M. Hutchins, The physics of violins, *Sci. Am.*, Vol. 207, pp. 79-93 (1962).

[3] J.C. Schelleng, The violin as a circuit, *J. Acoust. Soc. Am.,* Vol. 35, pp. 326-338 (1963); cf. erratum, p. 1291.

[4] C.M. Hutchins, A 30-year experiment in the acoustical and musical development of violin-family instruments, *J. Acoust. Soc. Am.,* Vol. 92, pp. 639-650 (1992).

[5] H. Dünnwald, Deduction of objective quality parameters on old and new violins, *Catgut Acoust. Soc. J.,* Vol. 1, No. 7 (Series II), pp. 1-5 (1991).

[6] M. Schleske, Eigenmodes of vibration in the working process of a violin, *Catgut Acoust. Soc. J.,* Vol. 3, No.1 (Series II), pp. 2-8 (1996).

[7] G. Bissinger and A. Gregorian, Relating normal mode properties of violins to overall quality: Signature modes, *Catgut Acoust. Soc. J.,* Vol. 4, No. 8 (Series II), pp. 37-45 (2003).

[8] G. Bissinger and C. Hutchins, Tuning the bass bar in a violin plate, *Catgut Acoust. Soc. Newsl.*, No. 26, pp. 10-12 (1976); No. 30, pp. 23-27 (1978).

[9] G. Bissinger, Some mechanical and acoustical consequences of the violin soundpost, *J. Acoust. Soc. Am.,* Vol. 97, pp. 3154-3164 (1995).

[10] K. Bird and M. J. Sherwin, *American Prometheus: The triumph and tragedy of J. Robert Oppenheimer* (Vintage Books, New York, 2006).

[11] C.M Hutchins, Founding a family of fiddles, *Phys. Today,* Vol. 20, pp. 23-27 (1967).

[12] J. Woodhouse, A set of test violins for player-rating experiments, *Proc. Stockholm Music. Acoust. Conf.*, Royal Swed. Acad. Mus., Vol. 79, pp. 438-440 (1993).

[13] I.-P. Beldie, Chladnische figuren und eigentone der geigenplatten, *Instrumenten-bau Zeitschrift,* Vol. 23, pp. 168-174 (1969); Engl. transl. repr. as Chladni figures and eigentones in violin plates, in *Musical Acoustics, Part II, Violin Family Functions*, C.M. Hutchins, ed. (Dowden, Hutchinson & Ross, Stroudsburg, PA, 1976).